

Investigating cross-orientation inhibition with continuous tracking

Pierfrancesco Ambrosi

Department of Neuroscience, Psychology,
Pharmacology, and Child Health,
University of Florence, Florence, Italy
IRCCS Stella Maris, Pisa, Italy



David Charles Burr

Department of Neuroscience, Psychology,
Pharmacology, and Child Health,
University of Florence, Florence, Italy
School of Psychology, University of Sydney,
Sydney, NSW, Australia



Maria Concetta Morrone

IRCCS Stella Maris, Pisa, Italy
Department of Translational Research in Medicine,
University of Pisa, Pisa, Italy



We investigated cross-orientation inhibition with the recently developed continuous tracking technique. We designed an experiment where participants tracked the horizontal motion of a narrow vertical grating. The target was superimposed on one of three different backgrounds, in separate sessions: a uniform gray background or a sinusoidal grating oriented either parallel or orthogonal to the target. Both mask and target where phase reversed. We cross-correlated target and mouse movements and compared the peaks and lags of response with the different masks. Our results are in agreement with previous findings on cross-orientation inhibition: The orthogonal mask had a weak effect on the peaks and lags of correlation as a function of target contrast, consistently with a divisive effect of the mask, while the parallel mask acted subtractively on the response. Interestingly, lags of correlation decreased approximately linearly with contrast, with decrements of the order of 100 ms, even at 10 times the detection threshold, confirming that it is possible to investigate behavioral differences above threshold using the continuous tracking paradigm.

provides information on perceptual sensitivity, as it affects target saliency and performance (Ambrosi, Burr, & Cicchini, 2022; Ambrosi, Pomè, & Burr, 2021; Bhat, Cicchini, & Burr, 2018; Bonnen, Burge, Yates, Pillow, & Cormack, 2015; Bonnen, Huk, & Cormack, 2017; Cormack, 2019; Huk, Bonnen, & He, 2018; Knoll, Pillow, & Huk, 2018; Mulligan, 2002; Mulligan, Stevenson, & Cormack, 2013; Straub & Rothkopf, 2022). Importantly, the continuous response includes information about the dynamics of responses, which may lead to a deeper understanding of the underlying perceptual mechanisms.

Continuous tracking might be useful to investigate behavioral consequences of neural phenomena that are mostly present above threshold or do not affect discrimination thresholds. One such example is cross-orientation inhibition (XOI), the mutual inhibitory processes between neurons in primary visual cortex (Burr, Morrone, & Maffei, 1981; Morrone, Burr, & Maffei, 1982). Primary visual cortex neurons are selectively tuned to orientation (Hubel & Wiesel, 1962), responding best to visual stimuli of a preferred orientation. However, they are also affected by the simultaneous presentation of a second, differently oriented stimulus, which by itself would not elicit any response (Bonds, 1989; Brouwer & Heeger, 2011; Burr & Morrone, 1987; DeAngelis, Robson, Ohzawa, & Freeman, 1992; Morrone & Burr, 1986; Morrone et al., 1982; Priebe, 2016; Priebe & Ferster, 2006; Snowden & Hammett, 1992). The nonoptimally

Introduction

Continuous tracking is a newly developed technique where participants track the position of a target stimulus moving on screen. The similarity between participant tracking and actual target trajectory

Citation: Ambrosi, P., Burr, D. C., & Morrone, M. C. (2024). Investigating cross-orientation inhibition with continuous tracking. *Journal of Vision*, 24(2):2, 1–17, <https://doi.org/10.1167/jov.24.2.2>.

<https://doi.org/10.1167/jov.24.2.2>

Received June 27, 2023; published February 1, 2024

ISSN 1534-7362 Copyright 2024 The Authors



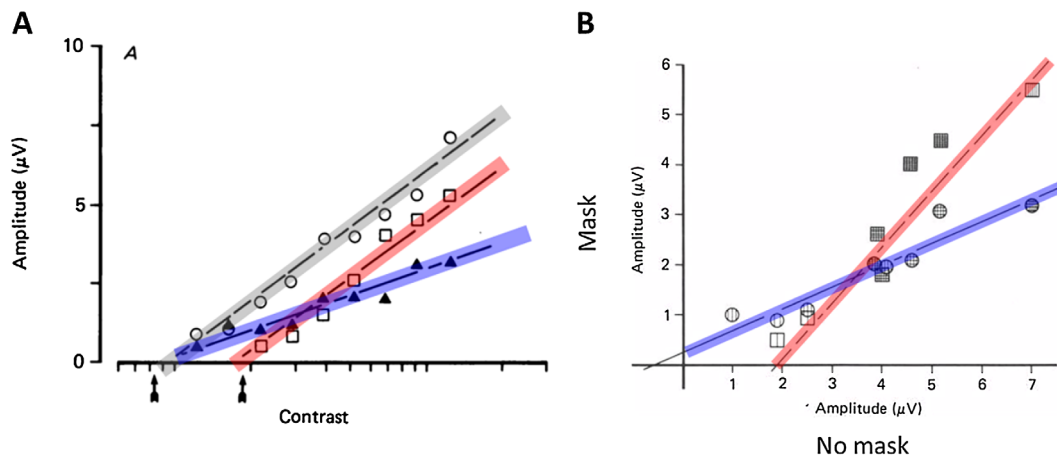


Figure 1. Plots taken from [Burr and Morrone \(1987\)](#). **(A)** Amplitude of VEP gain as a function of contrast. Target and masks were sinusoidal gratings, similar to those employed here. Symbols highlighted in gray, blue, and red are the gains measured with a gray background, orthogonal mask, or parallel mask, respectively. Arrows are detection thresholds. The orthogonal mask affects only the slope of the curve, the parallel mask only the intercept. **(B)** VEP gain amplitude with oriented masks plotted against those measured with the gray background. Since the orthogonal mask changes the slope, the resulting relationship, highlighted in blue, is linear with slope < 1 and intercept ~ 0 ; on the contrary, since the parallel mask changes the intercept, the relationship between the two is linear, with slope ~ 1 and intercept > 0 .

oriented stimulus reduces the response to the primary stimulus, in a divisive manner, while the effects of a parallel masking stimulus are subtractive. The main evidence in humans to date has come from visually evoked potentials (VEPs) ([Burr & Morrone, 1987](#); [Morrone & Burr, 1986](#); [Morrone et al., 1982](#)), blood oxygenation level dependent (BOLD) signals in functional MRI experiments ([Brouwer & Heeger, 2011](#)), and single-neuron recordings in cat ([Bonds, 1989](#); [Carandini, Heeger, & Movshon, 1997](#); [Morrone et al., 1982](#)). XOI is an important neural phenomenon because it should refine the orientation selectivity of visual neurons and might be important in regulating neural metabolic activity by normalizing neural response with respect to local image contrast ([Bonds, 1989](#); [DeAngelis et al., 1992](#)).

This phenomenon was first explained in terms of lateral inhibition from a large pool of cells, broadly tuned for orientation, in the primary visual cortex ([Burr & Morrone, 1987](#); [Morrone & Burr, 1986](#); [Morrone et al., 1982](#)), but later studies suggested that feed-forward inputs from the lateral geniculate nucleus (LGN) to primary cortex may also be involved ([Freeman, Durand, Kiper, & Carandini, 2002](#); [Li, Thompson, Duong, Peterson, & Freeman, 2006](#); [Priebe, 2016](#); [Priebe & Ferster, 2006](#)).

[Burr and Morrone \(1987\)](#) measured psychophysically detection thresholds and recorded VEPs in humans using sinusoidal gratings superimposed on masks of the same or different orientation. They found that compared with the target-only condition, detection thresholds were unaffected by the orthogonal masks but increased with the parallel masks. VEPs showed

that this effect is divisive: The orthogonal mask reduces the slope of the VEP gain as a function of contrast, while the parallel mask only shifts the curve vertically, indicating a subtractive response ([Figure 1](#)).

The fact that orthogonal mask inhibition is divisive suggested that normalization processes are involved in cross-orientation inhibition ([Carandini & Heeger, 2012](#); [Carandini, Heeger, & Senn, 2002](#); [Heeger, 1992](#)), possibly through changes in electrical conductance at the synapses ([Carandini & Heeger, 1994](#); [Carandini et al., 1997](#)), but mixed evidence has been found for this interpretation ([Carandini & Heeger, 2012](#)). Cross-orientation inhibition seems to be mediated by the GABAergic inhibitory system, because antagonists of the GABA_A-mediated inhibition reduce cross-orientation inhibition ([Morrone, Burr, & Speed, 1987](#)).

Psychophysically, an orthogonally oriented mask causes a much smaller (1–3 dB) increase in detection thresholds than a masking stimulus parallel to the target ([Campbell & Kulikowski, 1966](#); [Foley, 1994](#); [Meese & Holmes, 2007](#)), and in many conditions, XOI does not cause threshold elevation at all ([Burr & Morrone, 1987](#); [Morrone & Burr, 1986](#)). Since the continuous tracking paradigm measures participant responses dynamically, not just detection thresholds, it might be possible to reveal effects of orthogonal masks psychophysically.

We designed an experiment where participants tracked the horizontal motion of a vertical Gaussian-windowed grating (target stimulus). The target was temporally interleaved with one of three different masks, in separate sessions: a uniform gray background or a phase-reversing sinusoidal grating oriented either

parallel or orthogonal to the target. We cross-correlated target and mouse movements and compared the peaks and lags of response with the different masks. The results broadly confirm previous findings on cross-orientation inhibition using physiological techniques and provide interesting information about the dynamics of the process. The cross-correlation analysis revealed that lags of correlation decrease substantially above the detection threshold. It also suggested that the orthogonal mask might have a divisive effect on the peaks and lags of correlation and the parallel mask a subtractive effect.

Methods

Participants

Seven volunteers (aged 23–31 years, five females) were recruited, all with normal or corrected-to-normal vision. All participants had prior experience in psychophysical experiments, but only one had prior knowledge about the details of the experiment (author PA). All were right-handed and used their right hand for tracking. Experimental procedures are in line with the Declaration of Helsinki and were approved by the regional ethics committee (Comitato Etico Pediatrico Regionale, Azienda Ospedaliero-Universitaria Meyer, Florence, Italy). Written informed consent was obtained from each participant.

Stimuli

Stimuli were generated with MATLAB (MathWorks, Natick, MA, USA) and displayed on a Barco Calibrator monitor (CDCT 6551) 42×32 cm with mean luminance of 28 Cd/m^2 , resolution of 960×640 pixels, and refresh rate of 100 Hz, driven by a VSG Visage graphic board (Cambridge Research Systems, Rochester, UK) under the control of a PC computer. A regular USB mouse was used to collect responses in the tracking experiment. In all experiments, participants were placed at a 57-cm distance from the screen, which covered a visual field of 20×16 degrees. The target was a vertical sinusoidal grating of 1 c/deg, and the contrast of the stimulus was modulated by a 3.1-Hz square wave, producing abrupt contrast reversals at 6.2 Hz, windowed by a vertical Gaussian bar of a standard deviation of 0.6 degrees. The carrier and window moved together rigidly. The target was temporally interleaved with either a gray background or a sinusoidal grating oriented parallel or orthogonal to it. The two oriented gratings had a root-mean-square (RMS) contrast of 20% (28.6% Michelson equivalent), spatial frequency of 0.8 cpd, and temporal frequency of 2.5 Hz. All stimuli had mean luminance of 28 Cd/m^2 .

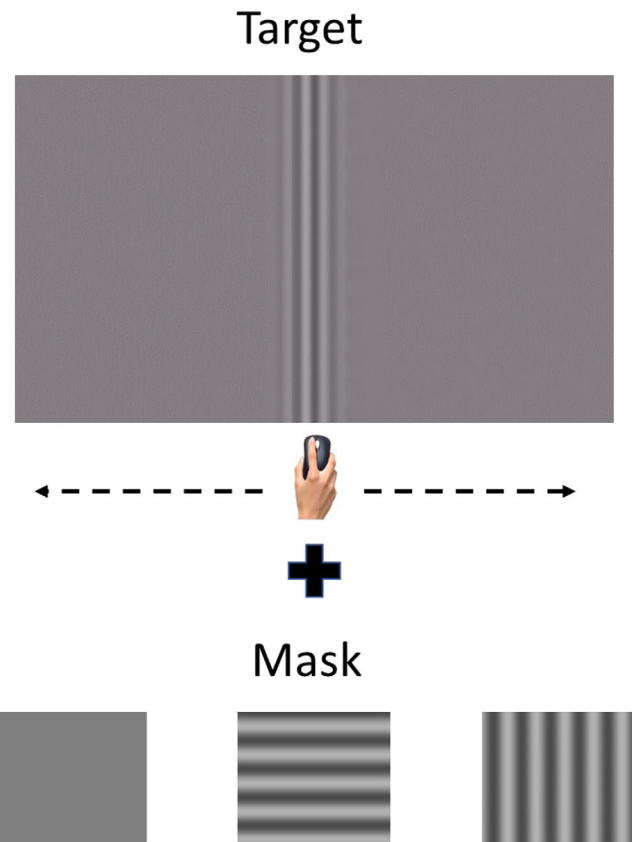


Figure 2. Example of the experimental procedure and stimuli. A vertical Gaussian-windowed grating (the target, top) moved horizontally in a random walk for 10 seconds. Participants followed its movements with a USB mouse. The target was temporally interleaved with one of the three masking stimuli shown at the bottom: a nonoriented gray background or a sinusoidal grating oriented horizontal or parallel to the target.

Examples of target and mask stimuli are shown in Figure 2. The target moved horizontally following a random walk, generated by choosing a new horizontal velocity from a random Gaussian distribution every 200 ms (20 frames), on average. To minimize autocorrelations, the updating frequency was jittered by ± 50 ms (five frames). This led to an average speed of 10 deg/s. In a second experiment, we decreased the mask contrast to 10% (14.3% Michelson) and doubled the temporal frequency of target and mask (6.2 and 5 Hz, respectively). Everything else was the same. This choice was made to reduce masking from the parallel mask, lowering threshold elevation, which allowed testing in a wider range of contrasts.

Experimental procedure

Participants were explicitly asked to “follow the horizontal displacements of the target with the mouse.” No visual feedback was shown on screen by cursor

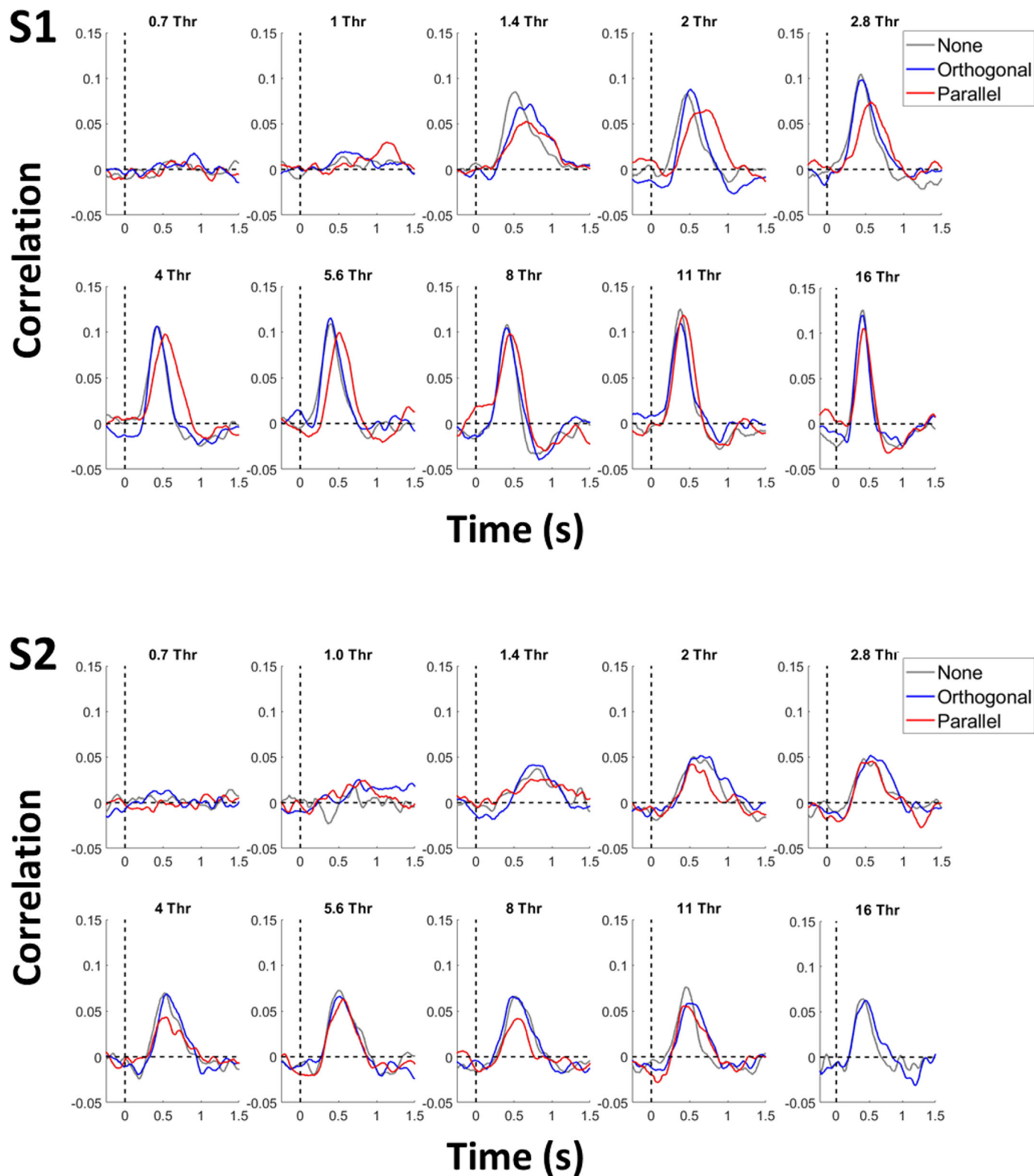


Figure 3. Results of the first tracking experiment on two of the four participants. Gray, blue, and red curves are the cross-correlations between target movements and mouse movements in the presence of the nonoriented, orthogonal, and parallel masks, respectively. In each panel, target contrast is a fixed multiple of each participant’s detection threshold for each mask, shown at the top of each panel.

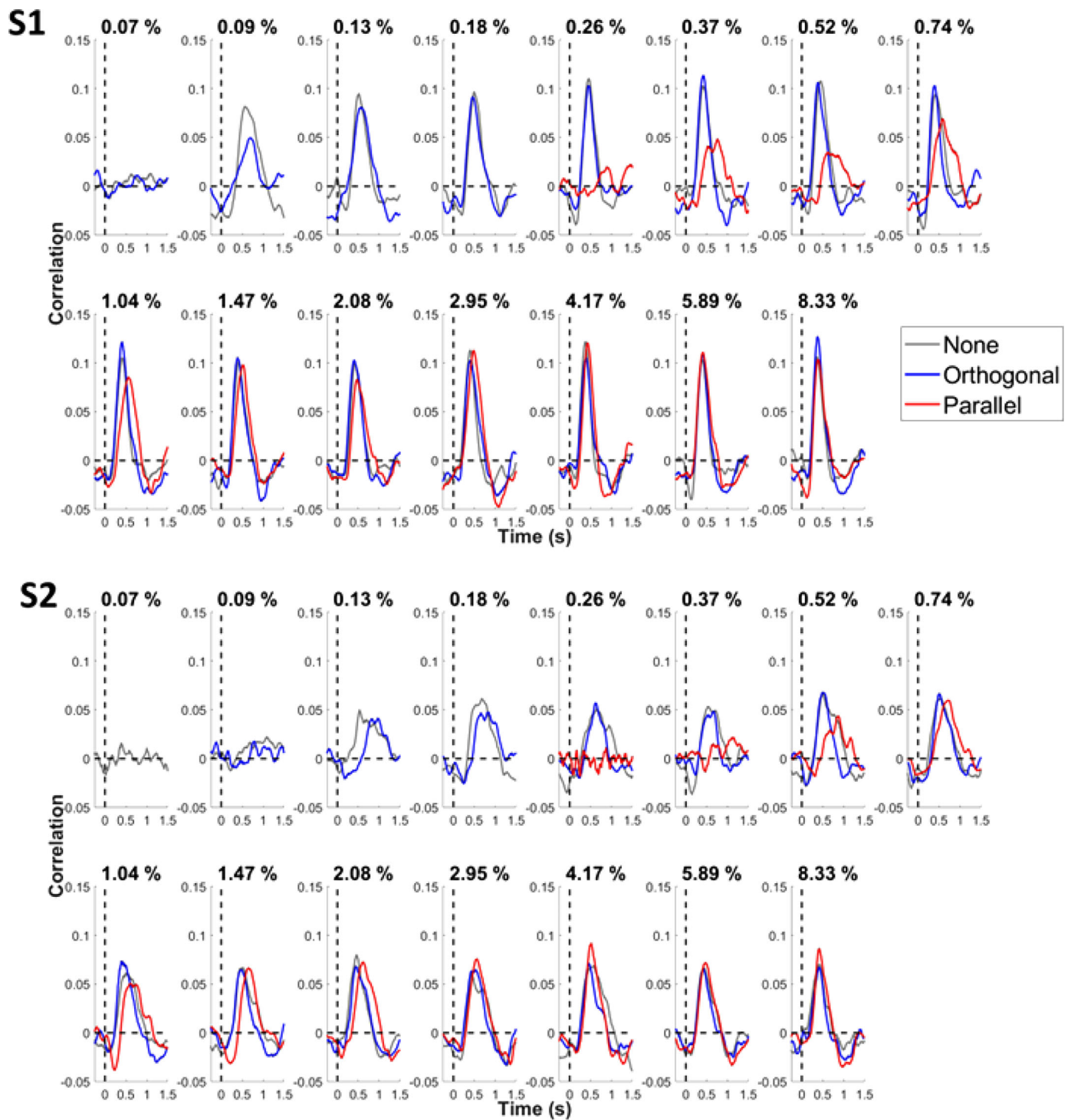


Figure 4. Results of the second tracking experiment on two of the four participants. Gray, blue, and red curves are the cross-correlations between target movements and mouse movements in the presence of the nonoriented, orthogonal, and parallel masks, respectively. Each panel shows results with the three backgrounds for a given target contrast, written at the top of each panel.

to prevent participants from using the displacement between features of the target and the cursor as a visual clue. Figure 2 shows a cartoon of the experimental procedure. In separate sessions, we varied the contrast of the target (between 0.06% and 8.3% standard

deviation of light intensities relative to the mean RMS contrast, which corresponds to 0.22% to 30% Michelson contrast), for each mask stimulus.

In the first experiment, all participants performed fifteen 10-second-long trials, for 10 different target

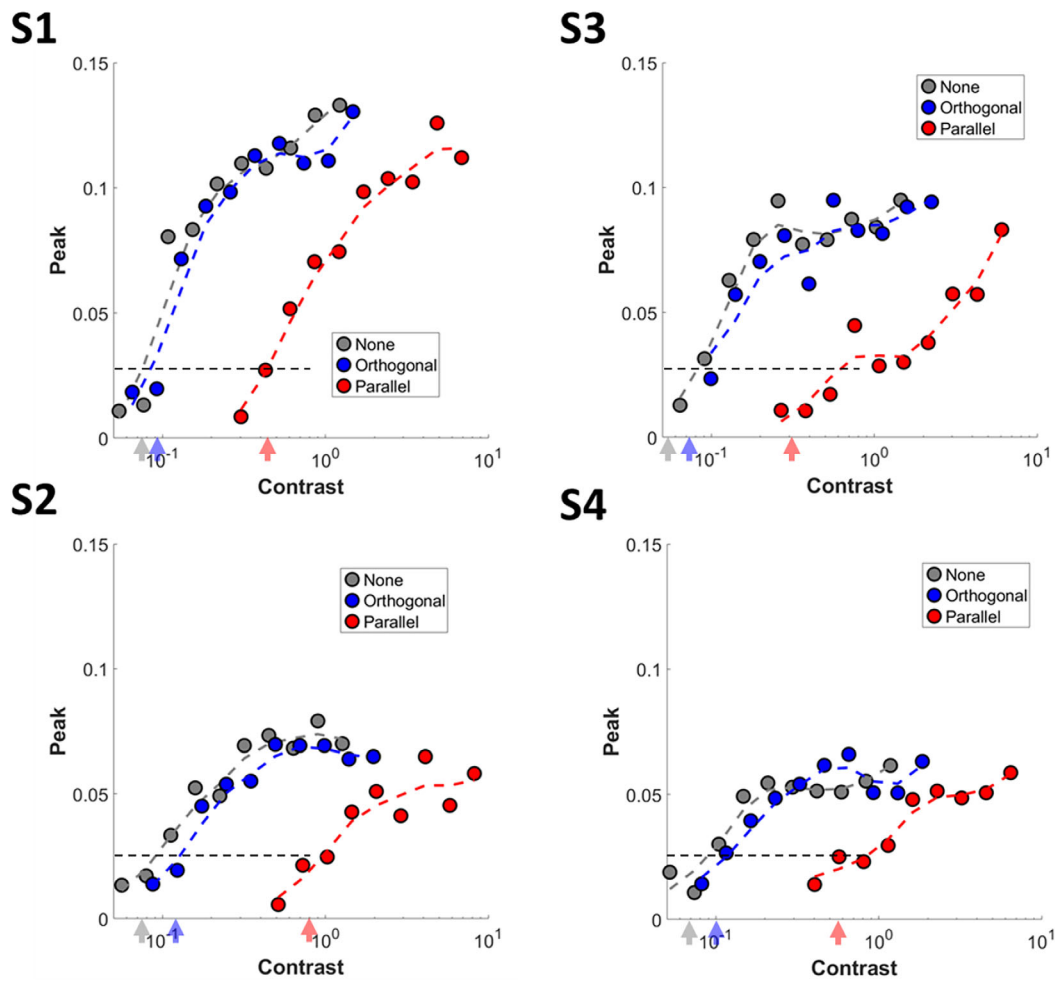


Figure 5. Results of the first tracking experiment on four participants. Peaks of correlation as a function of target percent RMS contrast (multiply by 3.67 for Michelson contrast), one panel for each participant. Gray, blue, and red symbols refer to the gray background, orthogonal mask, and parallel mask, respectively. The dashed colored curve is the smoothing of the data points (using a box car filter over five time steps), included to ease data visualization. Black dashed lines indicate the correlation value that was considered nonsignificant and excluded from the following analysis (compare with Figure 3; contrast conditions below the independently measured threshold were considered nonsignificant and excluded from the subsequent analysis). All participants were similarly affected by the two oriented masks: The parallel mask (red) shifts the curve laterally, while the orthogonal mask has little effect on the peaks of correlation. Arrows indicate the detection thresholds estimated as described in the Methods section, color coded as the peaks.

contrasts and three masks. In the second experiment, 15 target contrasts were tested, for each mask, and participants performed twelve 10-second-long trials. Participants S1, S2, and S3 participated in both experiments. Detection thresholds were estimated in a separate experiment: Participants had to adjust the contrast of a stimulus equal to the one used in the tracking experiment, but not moving, until it was barely visible.

Data analysis

We measured the normalized cross-correlation between target velocity and mouse velocity (displacements on each frame). Each target contrast

and mask condition were analyzed separately, averaging over all trials with the same target and mask. We estimated the peak and lag of each mean cross-correlogram by fitting its positive lobe with a Gaussian function and taking the peak and mean of the resulting curve. We then compared the peaks and lags of correlation as a function of contrast in presence of the different masks.

Results

Figures 3 and 4 show the results of the two tracking experiments with the three masks for two example

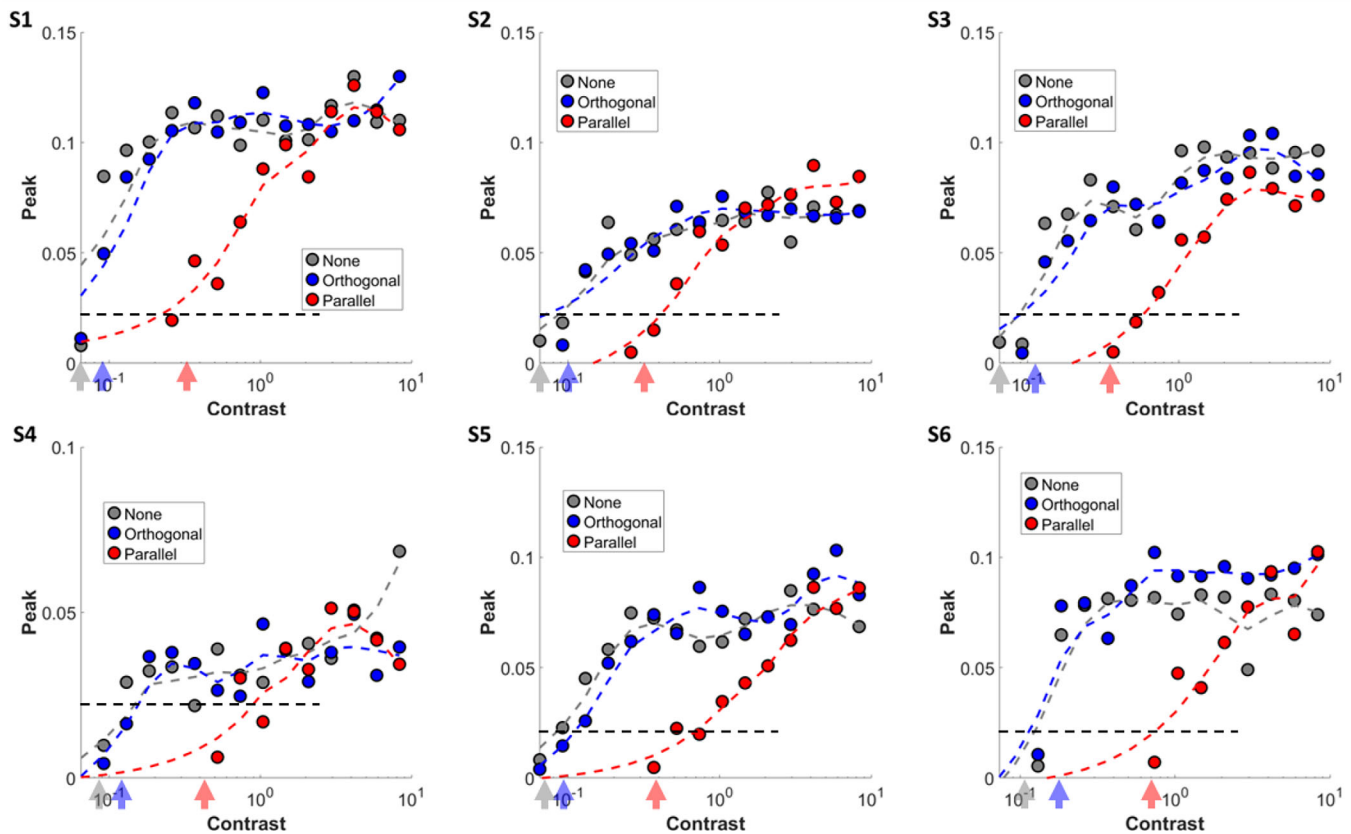


Figure 6. Results of the second tracking experiment on six participants. Peaks of correlation as a function of target RMS contrast, each panel for a different subject. Gray, blue, and red symbols refer to the gray background, orthogonal mask, and parallel mask, respectively. The dashed colored curve is the smoothing of the data points, included to ease data visualization. Black dashed lines indicate the correlation value that was considered nonsignificant and excluded from the following analysis (compare with Figure 4; nonsignificance was based on the separately measured detection thresholds). All participants were similarly affected by the two oriented masks: The parallel mask (red) shifts the curve laterally, while the orthogonal mask has little or no effect on the peaks of correlation. Arrows indicate the detection thresholds estimated as described in the Methods section, color coded as the peaks.

participants, S1 and S2. The results from the remaining participants are shown in the Appendix. Gray, blue, and red curves are the cross-correlograms obtained using the gray background, orthogonal mask, or parallel mask, respectively. Mask contrast was fixed for all participants in all conditions. First, we tested target contrasts that were fixed multiples of each participant's detection threshold. The ratio between target contrast and detection threshold is shown at the top of each panel of Figure 3. In the second round of acquisitions, participants were tested at fixed target contrasts for each mask, shown at the top of each panel of Figure 4. Contrast values are reported in RMS contrast, which can be converted to Michelson equivalent contrast by multiplying the RMS value by 3.67 for the targets and 1.43 for the masks.

The curves in Figures 3 and 4 show the cross-correlograms, obtained by correlating the velocity of the test stimuli with that of the mouse. In general, the function showed a strong positive peak, which we fitted

with a Gaussian function to estimate the peaks and lags of correlation. The main peak was often followed by a smaller negative peak, which may have been driven by corrective actions from participants. To test this, we compared the peaks of the negative lobes of the cross-correlogram with the peak of the nonnormalized cross-correlogram (Appendix C).

Figures 5 and 6 show the peaks of correlation as a function of target RMS contrast, on a logarithmic scale. Again, gray, blue, and red symbols refer to the gray background, orthogonal mask, and parallel mask conditions, respectively. Arrows indicate the detection thresholds, measured separately. The dependence of peaks of correlation on contrast is similar for all participants and for the different masks. For all participants, the orthogonal mask affected mildly the peaks of correlation, while the parallel mask increased the threshold and shifted horizontally the curve. We fitted the data with a Naka–Rushton function. These remained fairly constant across conditions. Only the

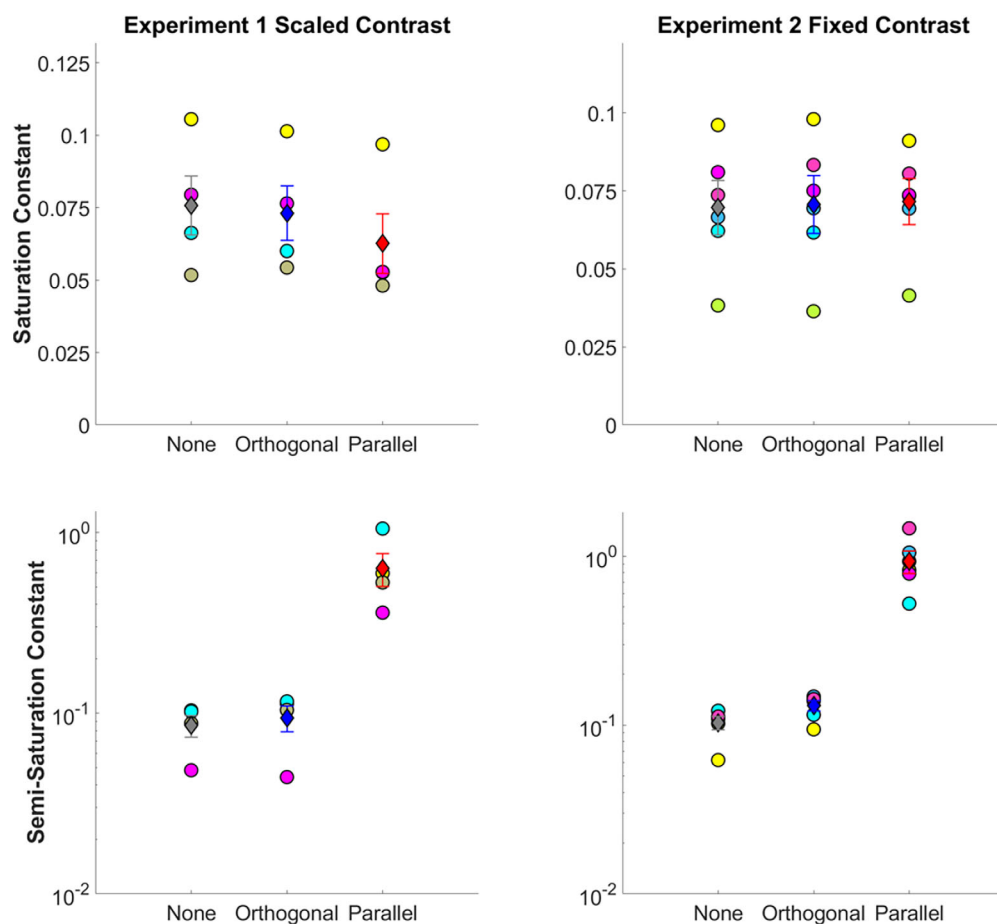


Figure 7. Results of the Naka–Rushton fits of the peak correlations as a function of contrast. Each participant is represented by a different color, the same in each panel and for participants who performed both experiments (S1, S2, and S3). Diamonds are averages across participants, and error bars are *SEM*, color coded as in previous figures. In all cases, results were significantly different from zero; that is, the confidence interval of each parameter did not include zero. The only parameter that is consistently and significantly different across masks is the semi-saturation constant in the presence of the parallel mask (bottom panels). This can be expected from the threshold elevation in the presence of subtractive effects.

semi-saturation constant was significantly different for the parallel mask condition, as would be expected from threshold elevations found with traditional psychophysics (Figure 7).

Figures 8 and 9 show the lags of correlation, with the same color scheme as previous figures. Notably, lags of correlation decreased with increasing target contrast, even when target contrasts were much higher than the detection threshold, for all masks: At contrasts 5 to 10 times the detection threshold, a five- or tenfold increase in target contrast caused a reduction in lags of correlation on the order of 100 ms. The orthogonal mask (blue) had a smaller effect on the lags of correlation than the parallel mask (red), but the two appeared to affect differently the lags of correlation: The parallel mask caused a steeper decrement of lags of correlation than the orthogonal mask, which affected only slightly the slope of the curve.

Figure 10 shows plots peaks and lags of correlation with the orthogonal (blue circles) and parallel (red circles) masks against those with the gray background. Panels A and B compare peaks and lags from Experiment 1, while panels C and D those from Experiment 2.

To compare across participants, we subtracted from each participant the mean value measured with the gray background condition. The black dashed lines are the equality lines. The blue and red lines are the linear fits of the data, with results reported in the insets. Interestingly, the results suggest a similar relationship to the expected: A slope < 1 and an intercept ~ 0 with the orthogonal mask and a slope ~ 1 and intercept $\neq 0$ with the parallel mask. This suggests that both peaks and lags of correlation with the orthogonal mask are lower than those obtained with the gray background. This means that even if peaks of correlation and accuracy

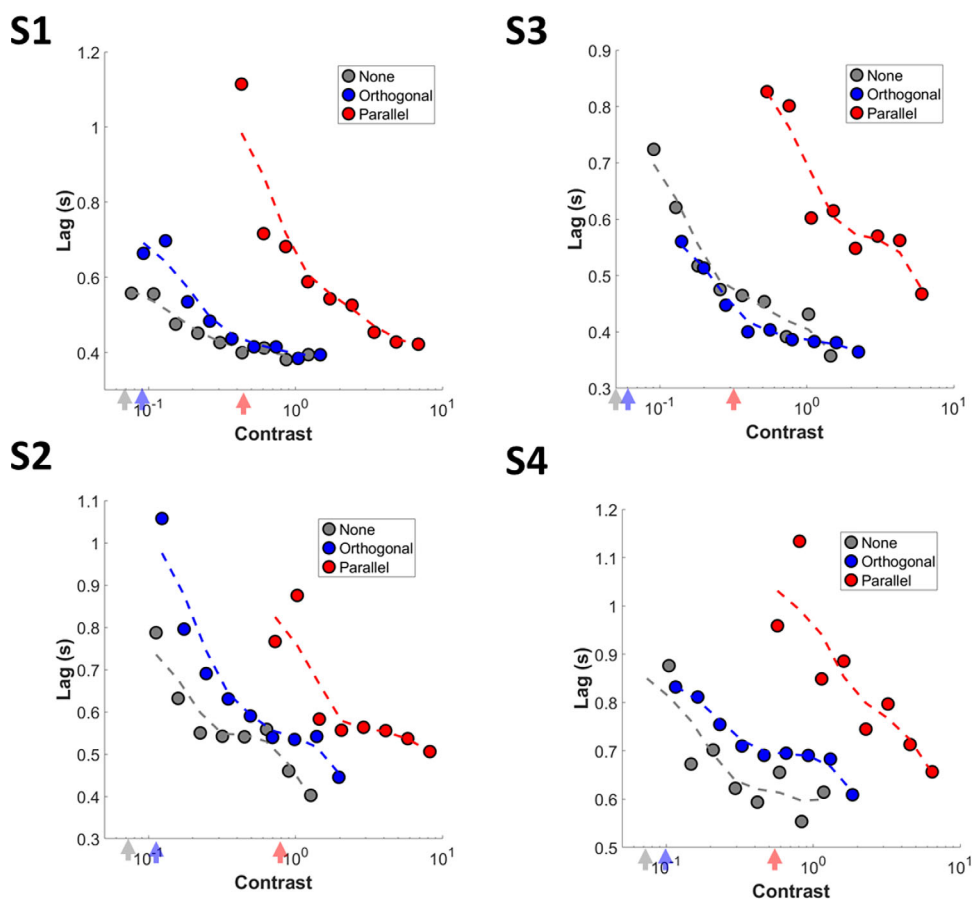


Figure 8. Results of the first tracking experiment on four participants. Lags of correlation, above contrast detection threshold (shown by the colored arrows), as a function of target RMS contrast for four subjects, color coded as in previous figures. Lags keep decreasing even for target contrasts largely above threshold. All participants are affected similarly by the oriented masks: The parallel mask strongly increases the lags of correlation; the orthogonal mask affects them only slightly.

are lowered by the orthogonal mask, participant responses are slightly faster in the presence of the orthogonal mask.

Discussion

In this experiment, we investigated psychophysically cross-orientation inhibition using continuous tracking. XOI is the inhibition in the response of neurons tuned to a specific stimulus orientation when the preferred stimulus is presented together with a second stimulus of different orientation, which would not itself elicit a response when presented in isolation (Brouwer & Heeger, 2011; Burr & Morrone, 1987; Carandini et al., 1997; Morrone & Burr, 1986; Morrone et al., 1982). The inhibition is largely divisive, as opposed to a subtractive effect of responses caused by a masking stimulus with similar orientation to the target.

We had participants track a vertically oriented target, superimposed on sinusoidal gratings oriented parallel or orthogonal to the target. The results show that peaks and lags of cross-correlation vary with contrast

in all mask conditions. Both parallel and orthogonal masks affected tracking responses, but parallel masks in general had a much stronger effect.

To understand better the effects of parallel and orthogonal masks, we plotted both the peak amplitudes and the lags of cross-correlograms obtained with superimposed masks against those of the no-mask conditions. The scatterplots were fit reasonably well by a linear function, especially the lags of cross-correlation. For peaks and lags, in both experiments, the effect of the parallel mask was to shift the best-fitting function rightward (indicating that higher contrasts were required for the parallel mask to match the no-mask performance). However, the effect of the orthogonal mask was to decrease slightly the slope of the fitted function, without affecting the intercept. These results suggest that the two masks affect differently tracking performance, consistent with the electrophysiological evidence (Figure 1) of the orthogonal mask acting divisively, changing the slopes of the response, and the parallel mask acting subtractively, causing the difference in the intercepts.

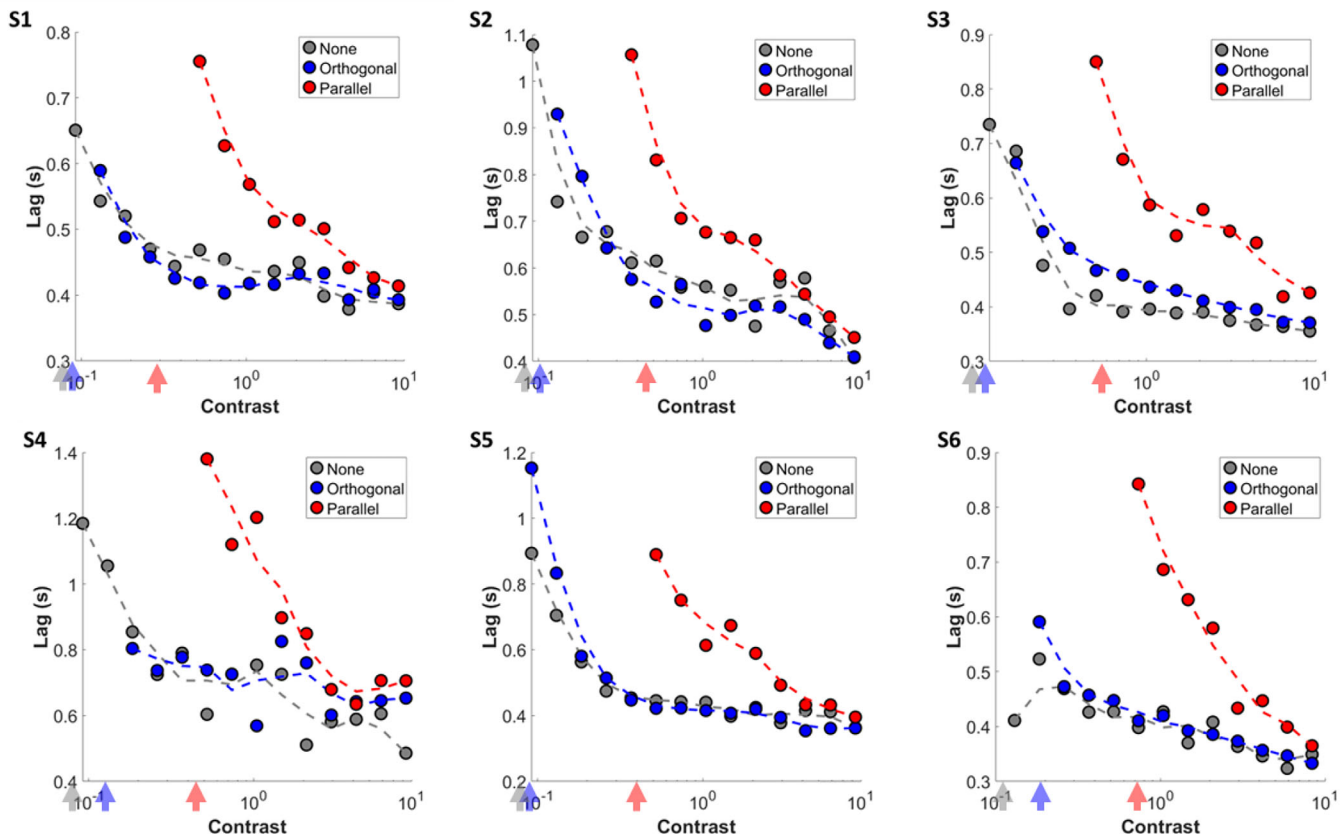


Figure 9. Experiment 2: Lags of correlation, above contrast detection threshold (indicated by the colored arrows), as a function of target RMS contrast for six subjects, color coded as in previous figures. Lags seem to keep decreasing even for target contrasts largely above threshold. All participants are affected similarly by the oriented masks: The parallel mask strongly increases the lags of correlation; the orthogonal mask affects them only slightly, especially closer to threshold.

Interestingly, the results show that the orthogonal masks decrease slightly both the peaks and lags of correlation. The lower peaks of correlation suggest that tracking is less precise with orthogonal masks. Lags of correlation, which are generally higher with lower peaks of correlation, are also lower (implying a faster response). In other words, participant responses appear to be slightly faster, but less accurate, when the orthogonal mask is present. It is tempting to relate this effect to the reduction of neuronal response caused by XOI, which in turn will drive the integration of visual information from low-level visual areas to functional areas involved in the detection of target motion and the implementation of the motor response. Interestingly, a phase advance between the no-mask and the orthogonal mask was also observed in single neuronal responses (Carandini et al., 1997) and in VEPs (Burr & Morrone, 1987), consistent with the above interpretation of the results.

We were also interested in the negative lobes in the correlation. We correlated the magnitude of the nonnormalized peaks in the cross-correlograms with the magnitude of the negative lobes and found a significant correlation ($r = -0.33$; see Appendix C):

Participants who made larger movements had larger negative lobes in the cross-correlograms. This implies that the corrective movements were related to target movements, not due to physical constraint of the apparatus. What do the negative lobes represent? As participants had no visual feedback of the cursor, and the task was one-dimensional, they may have made automatic back-and-forth corrective movements, resulting in negative lobes of correlation. However, the current design does not allow for a more definitive explanation.

Finally, our data also reveal an interesting behavioral difference common to all masks: Even when target contrast is much higher than threshold, lags of correlation keep decreasing as target contrast is increased, with an approximately log-linear relationship with target contrast for high target contrast. This result is similar to that previously shown in humans with electroencephalogram (Burr & Morrone, 1987; Morrone & Burr, 1986) and more recently with electrocorticographic (ECoGs), which showed in V1 up to 200 ms from maximum to threshold contrast (Groen et al., 2022). This value is very close to the effect observed here by tracking, suggesting that the

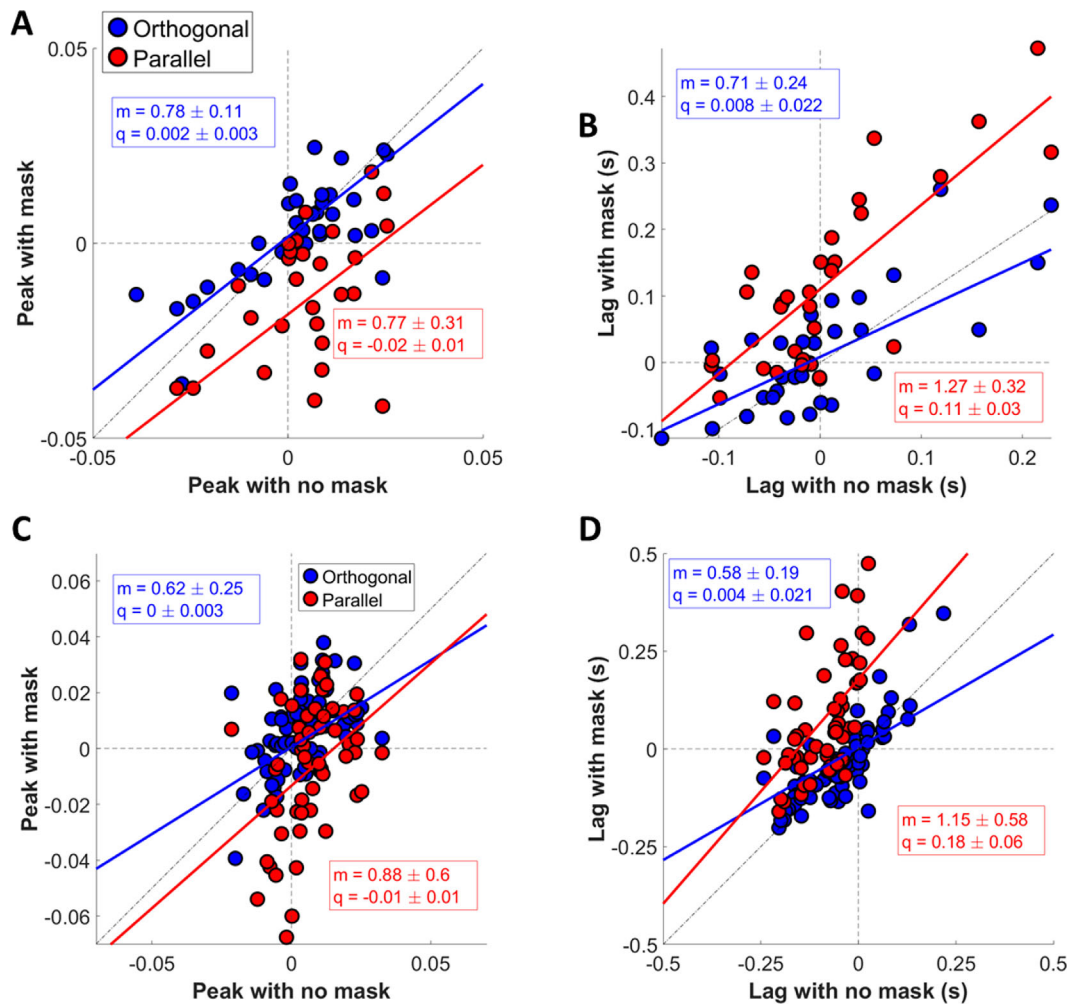


Figure 10. Peaks and lags of correlation measured with the two oriented masks plotted against the peaks and lags measured with the gray background, pooling across all participants. Blue symbols represent the results with the orthogonal mask, red ones those with the parallel mask. The insets report the results of linear fits of the data. Panels A and B show the comparison between peaks and lags of correlation with different masks from Experiment 1. Panels C and D show the comparison between peaks and lags from Experiment 2. The results of the linear fits, especially those for the lags of correlations B and D, are similar to the one shown in Figure 1: The slopes and intercepts of the data obtained with the orthogonal mask have a slope < 1 and an intercept close to 0, while those with the parallel mask have a slope of approximately 1 and an intercept different from 0.

possible interference due to motor delay and processing is negligible. The dependence on contrast was clear for all participants and for all masks, not specifically related to XOI.

The current study used a modern psychophysical technique to demonstrate the action of *cross-orientation inhibition*, suprathreshold interaction between orthogonal stimuli. The function of cross-orientation inhibition is still not completely determined, but most evidence suggests it relates to fine-tuning orientation selectivity of early visual cortex and may also reflect normalization mechanisms in visual processing (to take better advantage of the limited response range of neurons). The most robust available psychophysical technique is to measure

contrast thresholds, the minimum contrast to support detection: But as XOI is primarily a suprathreshold phenomenon, measuring differences in threshold does not always provide information about XOI. Other techniques, such as cross-orientation masking (Meese & Holmes, 2007), can be more suited to reveal suprathreshold differences, but they can be very time-consuming. Continuous tracking, on the other hand, is well suited to measure behavioral differences above threshold, while also providing much useful information about the temporal dynamics of the process.

Keywords: continuous psychophysics, cross-orientation inhibition, orientation tuning

Acknowledgments

Supported by the European Research Council (ERC) under the European Union's Horizon 2020 research and innovation program, Grant No. 832813 (GenPercept).

Commercial relationships: none.

Corresponding author: David Charles Burr.

Email: davidcharles.burr@in.cnr.it.

Address: Department of Neuroscience, Psychology, Pharmacology, and Child Health, University of Florence, Padiglione 26, Via di San Salvi, 26, Florence 50135, Italy.

References

- Ambrosi, P., Burr, D. C., & Cicchini, G. M. (2022). Ideal observer analysis for continuous tracking experiments. *Journal of Vision*, 22(2), 3, <https://doi.org/10.1167/jov.22.2.3>.
- Ambrosi, P., Pomè, A., & Burr, D. C. (2021). The dynamics of grouping-induced biases in apparent numerosity revealed by a continuous tracking technique. *Journal of Vision*, 21(13), 8, <https://doi.org/10.1167/jov.21.13.8>.
- Bhat, A., Cicchini, G. M., & Burr, D. C. (2018). Inhibitory surrounds of motion mechanisms revealed by continuous tracking. *Journal of Vision*, 18(13), 7, <https://doi.org/10.1167/18.13.7>.
- Bonds, A. B. (1989). Role of inhibition in the specification of orientation selectivity of cells in the cat striate cortex. *Visual Neuroscience*, 2(1), 41–55.
- Bonnen, K., Burge, J., Yates, J., Pillow, J., & Cormack, L. K. (2015). Continuous psychophysics: Target-tracking to measure visual sensitivity. *Journal of Vision*, 15(3), 14–14, <https://doi.org/10.1167/15.3.14>.
- Bonnen, K., Huk, A. C., & Cormack, L. K. (2017). Dynamic mechanisms of visually guided 3D motion tracking. *Journal of Neurophysiology*, 118(3), 1515–1531.
- Brouwer, G. J., & Heeger, D. J. (2011). Cross-orientation suppression in human visual cortex. *Journal of Neurophysiology*, 106(5), 2108–2119.
- Burr, D. C., & Morrone, M. C. (1987). Inhibitory interactions in the human vision system revealed in pattern-evoked potentials. *Journal of Physiology*, 389, 1–21.
- Burr, D. C., Morrone, M. C., & Maffei, L. (1981). Intra-cortical inhibition prevents simple cells from responding to textured visual patterns. *Experimental Brain Research*, 43(3–4), 455–458.
- Campbell, F. W., & Kulikowski, J. J. (1966). Orientational selectivity of the human visual system. *Journal of Physiology*, 187(2), 437–445.
- Carandini, M., & Heeger, D. J. (1994). Summation and division by neurons in primate visual cortex. *Science*, 264(5163), 1333–1336.
- Carandini, M., & Heeger, D. J. (2012). Normalization as a canonical neural computation. *Nature Reviews Neuroscience*, 13(1), 51–62.
- Carandini, M., Heeger, D. J., & Movshon, J. A. (1997). Linearity and normalization in simple cells of the macaque primary visual cortex. *Journal of Neuroscience*, 17(21), 8621–8644.
- Carandini, M., Heeger, D. J., & Senn, W. (2002). A synaptic explanation of suppression in visual cortex. *Journal of Neuroscience*, 22(22), 10053–10065.
- Cormack, L. (2019). Dynamics of motion induced position shifts revealed by continuous tracking. *Vision Sciences Society Annual Meeting Abstract*, 19, 294c.
- DeAngelis, G. C., Robson, J. G., Ohzawa, I., & Freeman, R. D. (1992). Organization of suppression in receptive fields of neurons in cat visual cortex. *Journal of Neurophysiology*, 68(1), 144–163.
- Foley, J. M. (1994). Human luminance pattern-vision mechanisms: Masking experiments require a new model. *Journal of the Optical Society of America A: Optics and Image Science*, 11(6), 1710–1719.
- Freeman, T. C., Durand, S., Kiper, D. C., & Carandini, M. (2002). Suppression without inhibition in visual cortex. *Neuron*, 35(4), 759–771.
- Groen, I. I. A., Piantoni, G., Montenegro, S., Flinker, A., Devore, S., Devinsky, O., . . . Winawer, J. (2022). Temporal dynamics of neural responses in human visual cortex. *Journal of Neuroscience*, 42(40), 7562–7580.
- Heeger, D. J. (1992). Normalization of cell responses in cat striate cortex. *Visual Neuroscience*, 9(2), 181–197.
- Hubel, D. H., & Wiesel, T. N. (1962). Receptive fields, binocular interaction and functional architecture in the cat's visual cortex. *Journal of Physiology*, 160, 106–154.
- Huk, A., Bonnen, K., & He, B. J. (2018). Beyond trial-based paradigms: Continuous behavior, ongoing neural activity, and natural stimuli. *Journal of Neuroscience*, 38(35), 7551–7558.
- Knoll, J., Pillow, J. W., & Huk, A. C. (2018). Lawful tracking of visual motion in humans, macaques, and marmosets in a naturalistic, continuous, and untrained behavioral context. *Proceedings of the National Academy of Sciences of the United States of America*, 115(44), E10486–E10494.

- Li, B., Thompson, J. K., Duong, T., Peterson, M. R., & Freeman, R. D. (2006). Origins of cross-orientation suppression in the visual cortex. *Journal of Neurophysiology*, 96(4), 1755–1764.
- Meese, T. S., & Holmes, D. J. (2007). Spatial and temporal dependencies of cross-orientation suppression in human vision. *Proceedings of the Royal Society B: Biological Sciences*, 274(1606), 127–136.
- Morrone, M. C., & Burr, D. C. (1986). Evidence for the existence and development of visual inhibition in humans. *Nature*, 321(6067), 235–237.
- Morrone, M. C., Burr, D. C., & Maffei, L. (1982). Functional implications of cross-orientation inhibition of cortical visual cells. I. Neurophysiological evidence. *Proceedings of the Royal Society B: Biological Sciences*, 216(1204), 335–354.
- Morrone, M. C., Burr, D. C., & Speed, H. D. (1987). Cross-orientation inhibition in cat is GABA mediated. *Experimental Brain Research*, 67(3), 635–644.
- Mulligan, J. B. (2002). Sensory processing delays measured with the eye-movement correlogram. *Annals of the New York Academy of Sciences*, 956, 476–478.
- Mulligan, J. B., Stevenson, S. B., & Cormack, L. K. (2013). *Reflexive and voluntary control of smooth eye movements. Paper presented at the Human Vision and Electronic Imaging XVIII, 4–8 February 2013, Burlingame, California, USA.*
- Priebe, N. J. (2016). Mechanisms of orientation selectivity in the primary visual cortex. *Annual Review of Vision Science*, 2, 85–107.
- Priebe, N. J., & Ferster, D. (2006). Mechanisms underlying cross-orientation suppression in cat visual cortex. *Nature Neuroscience*, 9(4), 552–561.
- Snowden, R. J., & Hammett, S. T. (1992). Subtractive and divisive adaptation in the human visual system. *Nature*, 355(6357), 248–250.
- Straub, D., & Rothkopf, C. A. (2022). Putting perception into action with inverse optimal control for continuous psychophysics. *Elife*, 11, e76635, <https://doi.org/10.7554/eLife.76635>.

Appendix A: Cross-correlograms from Experiment 1

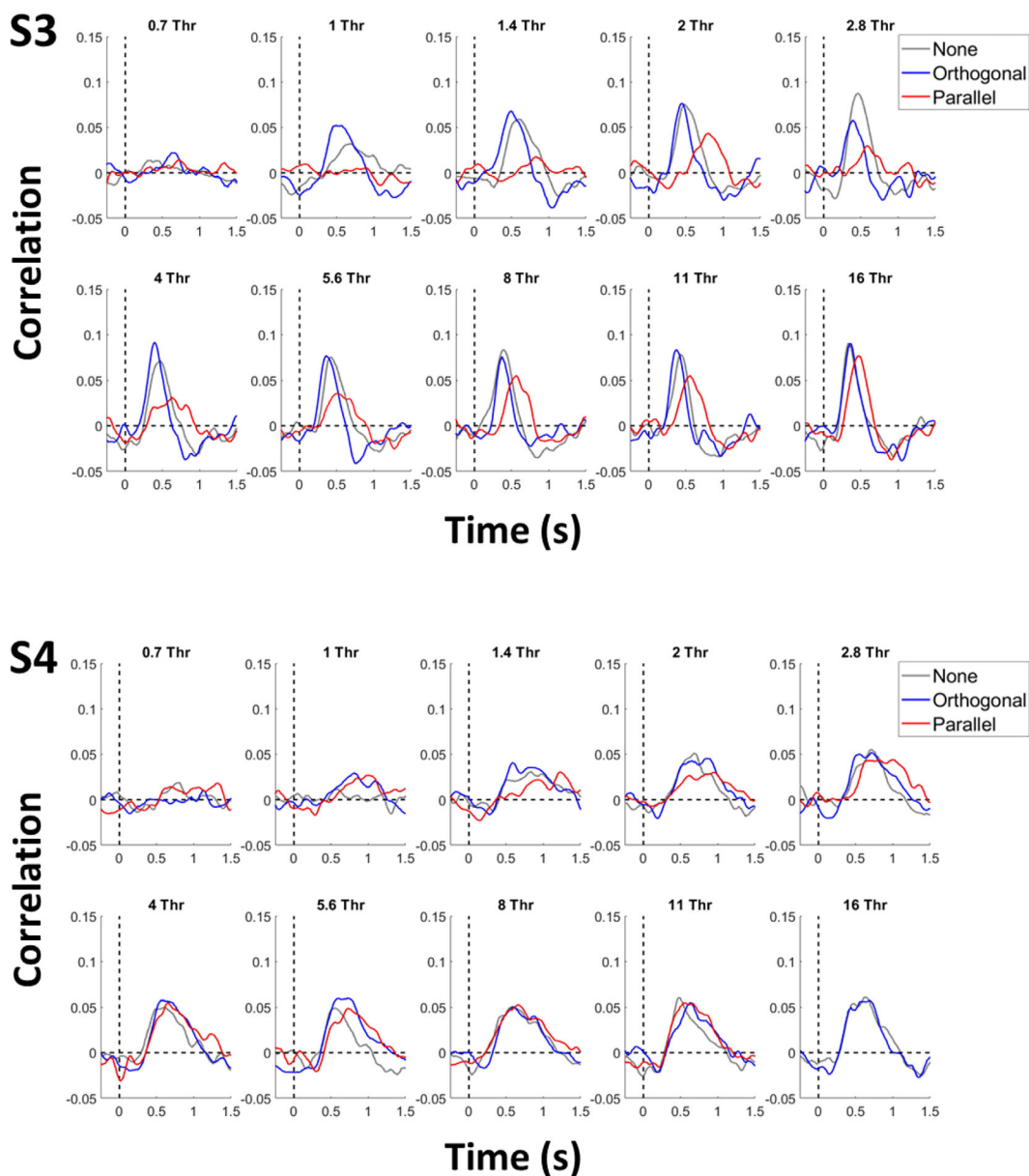


Figure A1. Results of the first tracking experiment on the remaining two participants. Gray, blue, and red curves are the cross-correlations between target movements and mouse movements in the presence of the nonoriented, orthogonal, and parallel masks, respectively. In each panel, target contrast is a fixed multiple of each participants' detection threshold for each mask, shown at the top of each panel.

Appendix B: Cross-correlograms from Experiment 2

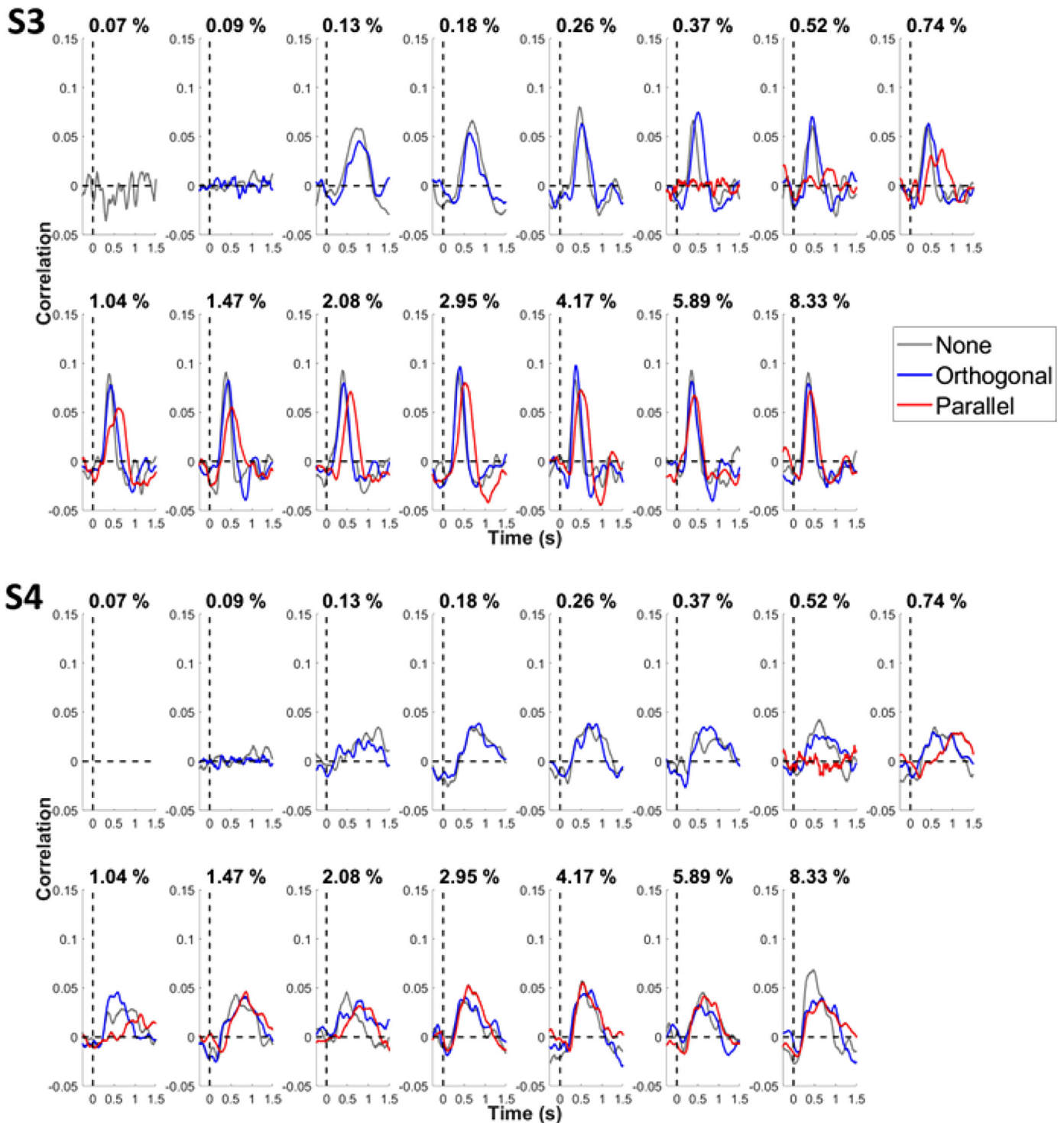


Figure B1. Results of the second tracking experiment on six participants. Gray, blue, and red curves are the cross-correlations between target movements and mouse movements in presence of the nonoriented, orthogonal, and parallel masks, respectively. Each panel shows results with the three backgrounds for a given target contrast, written on top of each panel.

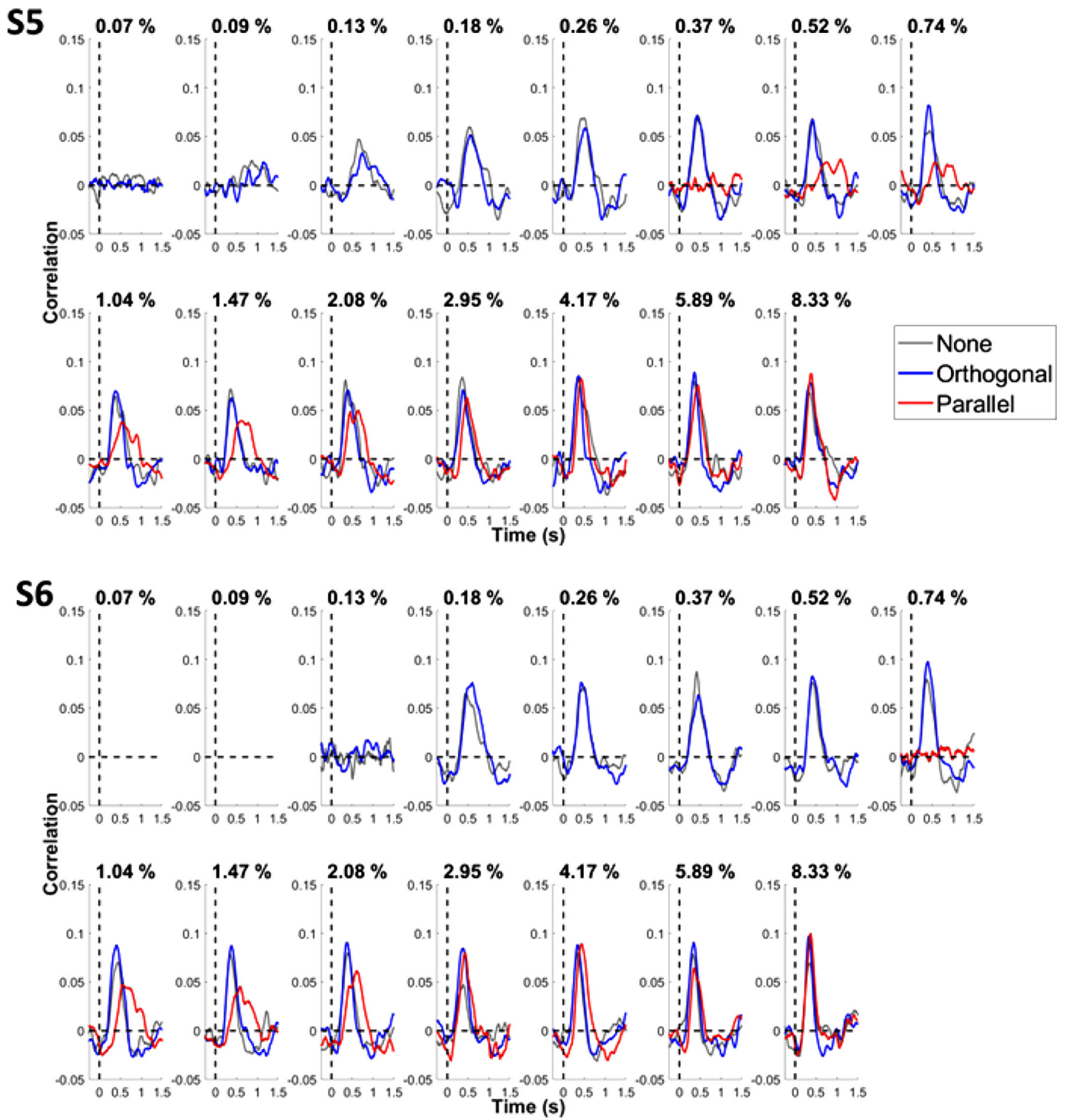


Figure B2. Continued.

Appendix C: Negative lobes of correlation

The positive lobe of the cross-correlogram was often followed by a smaller negative peak, probably caused by corrective actions from participants. To test this, we compared the peaks of the negative lobes of the cross-correlogram with the peak of the nonnormalized cross-correlograms. We did this because with the current setup, it was not possible to directly compare mouse and target position, as the participant had no visual feedback from the cursor, and because the cursor was controlled to prevent it from stopping at the edge of the screen, constrained within a rectangular portion of the screen and recentered when the border of this region was reached. Its position was cumulatively registered as if no recentering was made. These precautions were adopted to allow free motion of the mouse. However, since all participants were tested on the same apparatus, comparing peaks of nonnormalized cross-correlation between target and mouse movements should allow testing if larger movements are associated with larger negative lobes. Peaks of negative lobes were fitted with Voigt functions of the following form:

$$V(t) = \frac{a}{t^2 + a^2} * e^{-((t-b)/c)^2}$$

and the maximum value of the fitted function was taken as the peak. Not all participants showed significant correlations between negative peaks and tracking

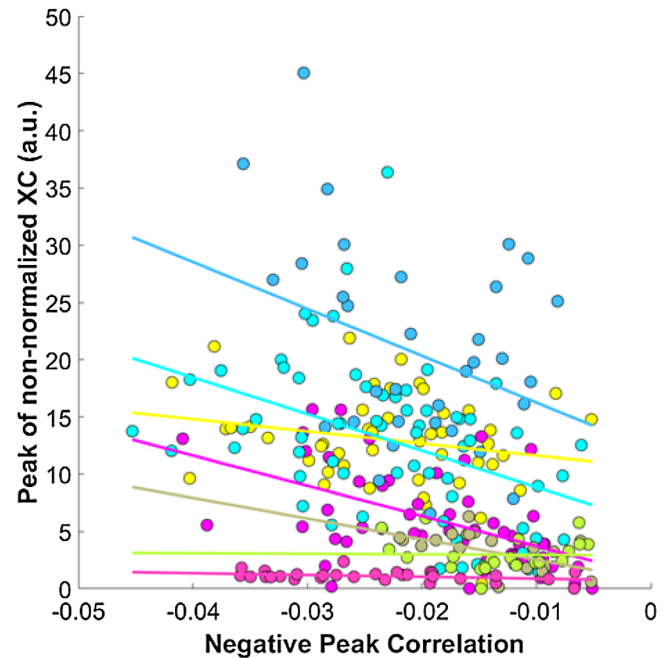


Figure C1. Negative peaks of correlation against peaks of nonnormalized correlations. Each color represents a different participant, and the same color is used for different experiments. Lines are linear fits of the data. A trend is visible for most participants taken separately, and the correlation between all data is significant ($r = -0.33$, $p < 10^{-3}$).

gain in each experiment taken separately, but the two measures were correlated when pooling across all data ($r = -0.33$, $p < 10^{-3}$).